NF- B/RelA and Nrf2 cooperate to maintain hepatocyte integrity and to prevent development of hepatocellular adenoma

Köhler, Ulrike A ; Böhm, Friederike ; Rolfs, Frank ; Egger, Michèle ; Hornemann, Thorsten ; Pasparakis, Manolis ; Weber, Achim ; Werner, Sabine

Abstract: BACKGROUND AND AIMS: The liver is frequently challenged by toxins and reactive oxygen species. Therefore, hepatocytes require cytoprotective strategies to cope with these insults. Since the transcription factors Nrf2 and NF- B regulate the cellular antioxidant defense system and important survival pathways, we determined their individual and overlapping functions in the liver. METHODS: We generated mice lacking Nrf2 and the NF- B RelA/p65 subunit in hepatocytes and we analyzed their liver using histopathology, immunohistochemistry, quantitative RT-PCR, Westernblot and Oxyblot analysis. Human inflammatory hepatocellular adenomas (iHCA) were analyzed by immunohistochemistry. RESULTS: Loss of either Nrf2 or NF- B/RelA had only a minor effect on liver homeostasis, but the double knockout mice spontaneously developed liver inflammation and fibrosis. Upon aging, more than one third of the female double mutant mice developed tumors, which histologically resemble human iHCA, a tumor that predominantly occurs in women. The mouse tumors also recapitulated the immunohistochemical marker profile characteristic for human iHCA. Moreover, pNRF2 and NF- B RelA/p65 was not detectable in the nuclei of iHCA tumor cells. The mouse phenotype was not due to a synergistic effect of both transcription factors on cytoprotective Nrf2 target genes. Rather, loss of Nrf2 or NF- B/RelA altered the expression of different genes, and the combination of these alterations likely affects liver homeostasis in the double mutant mice. CONCLUSIONS: Our results provide genetic evidence for a functional crosstalk of Nrf2 and NF- B/RelA in hepatocytes, which protects the liver from necrosis, inflammation and fibrosis. Furthermore, the double mutant mice represent a valuable animal model for iHCA.

DOI: https://doi.org/10.1016/j.jhep.2015.08.033

DOI: https://doi.org/10.1016/j.jhep.2015.08.033

Accepted Manuscript

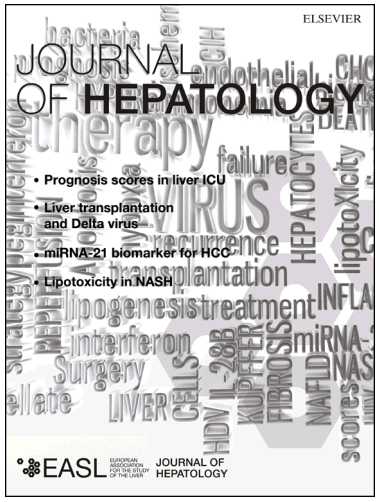

NF-κB/RelA and Nrf2 cooperate to maintain hepatocyte integrity and to prevent development of hepatocellular adenoma

Ulrike A. Köhler, Friederike Böhm, Frank Rolfs, Michèle Egger, Thorsten Hornemann, Manolis Pasparakis, Achim Weber, Sabine Werner

PII: S0168-8278(15)00613-3
DOI: http://dx.doi.org/10.1016/j.jhep.2015.08.033
Reference: JHEPAT 5820

To appear in: *Journal of Hepatology*

Received Date: 21 January 2015
Revised Date: 12 August 2015
Accepted Date: 31 August 2015

Please cite this article as: Köhler, U.A., Böhm, F., Rolfs, F., Egger, M., Hornemann, T., Pasparakis, M., Weber, A., Werner, S., NF-κB/RelA and Nrf2 cooperate to maintain hepatocyte integrity and to prevent development of hepatocellular adenoma, *Journal of Hepatology* (2015), doi: http://dx.doi.org/10.1016/j.jhep.2015.08.033

NF-κB/RelA and Nrf2 cooperate to maintain hepatocyte integrity and to prevent development of hepatocellular adenoma

Ulrike A. Köhler[1], Friederike Böhm[2], Frank Rolfs[1], Michèle Egger[2], Thorsten Hornemann[3], Manolis Pasparakis[4], Achim Weber[2*] and Sabine Werner[1*]

[1]Department of Biology, Institute of Molecular Health Sciences, Swiss Federal Institute of Technology (ETH) Zurich, 8093 Zurich, Switzerland

[2]Institute of Surgical Pathology, and [3]Institute of Clinical Chemistry, University of Zurich and University Hospital Zurich, 8091 Zurich, Switzerland

[4]Institute for Genetics, University of Cologne, 50674 Cologne, Germany

***Address for correspondence (joint corresponding and senior authors):**

Prof. Dr. Sabine Werner, Institute of Molecular Health Sciences, Otto-Stern-Weg 7, 8093 Zurich, Switzerland, Tel.: +41 44 633 3941; Fax: +41 44 633 1174, E-mail: Sabine.werner@biol.ethz.ch

Prof. Dr. Achim Weber, Institute of Surgical Pathology, University of Zurich and University Hospital of Zurich, Schmelzbergstrasse 12, 8091 Zurich, Switzerland, Tel.: 41 44 255 2781; E-mail: achim.weber@usz.ch

Electronic word count: 250 (abstract); 6294 (total)

Number of Figures: 7; number of Tables: 0

List of abbreviations

ALT: alanine transaminase

ARE: Antioxidant response element

AST: aspartate transaminase

BHA: Butylated hydroxyanisole

BrdU: 5-bromo-2'-deoxyuridine

FABP: Fatty acid binding protein

Gclc: Glutamate-cysteine ligase catalytic subunit

Gsta2: Glutathione S-transferase 2

Hmox1: Heme oxygenase 1

iHCA: Inflammatory hepatocellular adenoma

NADPH: Nicotinamide adenine dinucleotide phosphate

NF-κB: Nuclear factor κB

Nqo1: NADP(H) dehydrogenase, quinone 1

Nrf2: Nuclear factor erythroid 2-related factor 2

PBS: Phosphate-buffered saline

Prdx: Peroxiredoxin

ROS: Reactive oxygen species

SAA1: Serum amyloid A1

STAT3: Signal transducer and activator of transcription 3

TNF-α: Tumor necrosis factor α

Key words: Nrf2, NF-κB, hepatocellular adenoma, inflammation, liver fibrosis

Conflict of interest: None

Financial support: Supported by grants from ETH Zurich (No. 0-23123-08 to S.W.), the Swiss National Science Foundation (310030-142884 to S.W.), the Swiss Cancer League (KLS – 02773-02-2011 to A.W.), the Promedica Foundation Chur (to A.W.), and the Boehringer Ingelheim Fonds (predoctoral fellowship to U.A.K). U.A.K. was a member of the International Research Training Group (IRTG 1331; Konstanz/Zürich).

Authors' contributions: U.A.K, F.B., F.R., M.E. and T.H. performed the experiments, M.P. provided p65 knockout mice and initiated the study together with S.W., A.W. performed the histopathological analysis and coordinated the study together with S.W. S.W. wrote the manuscript together with U.A.K. and designed the study. All authors made important comments to the manuscript.

Abstract

Background and Aims: The liver is frequently challenged by toxins and reactive oxygen species. Therefore, hepatocytes require cytoprotective strategies to cope with these insults. Since the transcription factors Nrf2 and NF-κB regulate the cellular antioxidant defense system and important survival pathways, we determined their individual and overlapping functions in the liver.

Methods: We generated mice lacking Nrf2 and the NF-κB RelA/p65 subunit in hepatocytes and we analyzed their liver using histopathology, immunohistochemistry, quantitative RT-PCR, Westernblot and Oxyblot analysis. Human inflammatory hepatocellular adenomas (iHCA) were analyzed by immunohistochemistry.

Results: Loss of either Nrf2 or NF-κB/RelA had only a minor effect on liver homeostasis, but the double knockout mice spontaneously developed liver inflammation and fibrosis. Upon aging, more than one third of the female double mutant mice developed tumors, which histologically resemble human iHCA, a tumor that predominantly occurs in women. The mouse tumors also recapitulated the immunohistochemical marker profile characteristic for human iHCA. Moreover, pNRF2 and NF-κB RelA/p65 was not detectable in the nuclei of iHCA tumor cells. The mouse phenotype was not due to a synergistic effect of both transcription factors on cytoprotective Nrf2 target genes. Rather, loss of Nrf2 or NF-κB/RelA altered the expression of different genes, and the combination of these alterations likely affects liver homeostasis in the double mutant mice.

Conclusions: Our results provide genetic evidence for a functional cross-talk of Nrf2 and NF-κB/RelA in hepatocytes, which protects the liver from necrosis, inflammation and fibrosis. Furthermore, the double mutant mice represent a valuable animal model for iHCA.

Introduction

The liver's capability to regenerate completely after tissue loss induced by viruses, toxins or surgery is unique and astounding. Chronic liver damage, which occurs for example upon long-term alcohol abuse or viral hepatitis, however, limits the regenerative potential drastically. This may lead to the development of liver fibrosis, cirrhosis, and finally tumorigenesis and/or liver failure. It has been suggested that oxidative stress plays a central role in impaired liver regeneration and liver tumorigenesis [1-3]. Therefore, further understanding of the mechanisms controlling redox homeostasis in the liver may contribute to the development of new strategies to prevent or treat chronic liver disease and ultimately liver cancer.

A particularly important regulator of the cellular redox balance is nuclear factor erythroid 2-related factor 2 (Nrf2), a ubiquitously expressed member of the cap'n' collar family of transcription factors. Nrf2 activity is controlled by binding to the cytoplasmic inhibitory protein Keap1, which also mediates its ubiquitination and subsequent proteasomal degradation. Oxidation or covalent modifications of cysteine residues in Keap1 weaken the interaction with Nrf2, allowing its stabilization and nuclear accumulation. In the nucleus, Nrf2 dimerizes with a small Maf protein, followed by binding to antioxidant response elements (AREs) in enhancer or promoter regions of genes encoding various antioxidant proteins and detoxifying enzymes [4]. The central role of Nrf2 in cytoprotection is demonstrated by the phenotype of Nrf2-deficient mice. Although young mice do not display obvious abnormalities, they were highly susceptible to different toxins,

and they showed enhanced susceptibility towards chemical carcinogenesis in various organs, including the liver [5,6].

We and others previously demonstrated the requirement of Nrf2 for liver regeneration. Nrf2-deficient mice displayed oxidative stress in the liver that was aggravated after liver injury. In addition, liver regeneration after partial hepatectomy was impaired in Nrf2 knockout mice as a result of partial insulin/insulin-like growth factor 1 resistance caused by oxidative stress and/or of impaired Notch signaling [7,8]. Nrf2-deficiency also caused impaired repair of carbon tetrachloride-induced liver damage and concomitant enhancement of the pro-inflammatory and pro-fibrotic response [9]. Interestingly, Nrf2 knockout mice displayed enhanced DNA binding of nuclear factor κB (NF-κB) after partial hepatectomy [7]. This is most likely the consequence of the oxidative stress in Nrf2-deficient cells, as ROS have been shown to activate NF-κB [10]. Since cytoprotective functions of NF-κB in hepatocytes have been demonstrated, in particular under stress conditions [11,12], we speculated that the increased activity of NF-κB in the regenerating liver of Nrf2 knockout mice could at least in part compensate for the loss of Nrf2.

To test this possibility, we analyzed the consequences of a combined loss-of-function of Nrf2 and NF-κB in hepatocytes. For this purpose we decided to use mice with a hepatocyte-specific loss of the NF-κB subunit p65/RelA [13]. The RelA/p65-p50 dimer is the most abundant NF-κB heterodimer in canonical NF-κB signaling, and it regulates various genes involved in the control of apoptosis and

inflammation [14]. Mice lacking p65/RelA in hepatocytes show a severe reduction in total NF-κB activity, but due to the presence of other NF-κB family members they do not exhibit a phenotype in the non-challenged liver. However, they are highly susceptible to lipopolysaccharide- and tumor necrosis factor (TNF)-α-induced liver damage, respectively [13,15]. Interestingly, systemic treatment of these mice with the antioxidant butylated hydroxyanisole (BHA) prevented TNF-α-induced apoptosis in p65/RelA deficient hepatocytes [15]. BHA had previously been shown to induce the expression of cytoprotective Nrf2 target genes, including NAD(P)H dehydrogenase, quinone 1 (*Nqo1*) and heme oxygenase 1 (*Hmox-1*) as a consequence of direct Nrf2 activation [16,17]. This finding further suggests that Nrf2 and NF-κB have overlapping cytoprotective functions in the liver, and this hypothesis was experimentally confirmed *in vivo* in the present study.

Materials and Methods

Mice. *Nrf2* knockout mice [18] and mice homozygous for the floxed *p65/RelA* allele $p65^{fl}$ [13] were mated with homozygous Albumin-Cre (AlbCre) transgenic mice to obtain offspring heterozygous for *Nrf2* or $p65^{fl}$ and hemizygous for *AlbCre*. These $AlbCre^{tg/wt}$_$p65^{fl/wt}$ and $AlbCre^{tg/wt}$_$Nrf2^{ko/wt}$ mice were then crossed to generate $AlbCre^{tg/wt}$_$p65^{fl/fl}$ or $AlbCre^{tg/tg}$_$p65^{fl/fl}$ and $AlbCre^{tg/wt}$_$Nrf2^{ko/ko}$ or $AlbCre^{tg/tg}$_$Nrf2^{ko/ko}$ mice, respectively. Finally, these lines were crossed to obtain $AlbCre^{tg/wt}$_$p65^{wt/wt}$_ $Nrf2^{wt/wt}$ (here called AlbCre), $AlbCre^{tg/wt}$_$p65^{fl/fl}$_ $Nrf2^{wt/wt}$ (here called AlbCre_p65ko), $AlbCre^{tg/wt}$_$p65^{wt/wt}$_ $Nrf2^{ko/ko}$ (here called AlbCre_Nrf2ko), and $AlbCre^{tg/wt}$_$p65^{fl/fl}$_ $Nrf2^{ko/ko}$ animals (here called AlbCre_p65ko/Nrf2ko). All mice were in C57BL/6 genetic background.

Mice were housed and fed according to federal guidelines. They were free of pathogens. All animal experiments were performed with permission by the local veterinary authorities of Zurich, Switzerland.

Preparation of liver tissue. After euthanization of mice by CO_2 inhalation, blood was collected by cardiac puncture and liver tissue was harvested. For RNA isolation or preparation of protein lysates, liver samples were immediately frozen in liquid nitrogen and stored at -80 °C. For histology or immunohistochemistry liver samples were fixed in 4 % paraformaldehyde in phosphate-buffered saline (PBS) or in 95 % ethanol/1 % acetic acid and embedded in paraffin.

RNA isolation and quantitative RT-PCR (qRT-PCR). Isolation of RNA from murine liver was carried out as previously described [19]. cDNA synthesis was performed using the iScript RT kit (Biorad, Hercules, CA) according to the manufacturer's instructions. qRT-PCR was performed as described previously [20] using the primers listed in Supplementary Materials.

Preparation of protein lysates and Westernblot analysis. Liver samples were homogenized in T-PER^{TM} tissue protein extraction reagent (Pierce, Rockford, IL) supplemented with 0.1 U/ml aprotinin, 1 % leupeptin, 1 % pepstatin, 1 mM AEBSF, 10 mM sodium pyrophosphate, 1 mM sodium vanadate and 50 mM sodium fluoride. Lysates were cleared by sonication and centrifugation. Protein concentrations were determined with the BCA^{TM} Protein Assay Kit (Pierce). Proteins were separated by SDS-PAGE and transferred to nitrocellulose membranes. Unspecific binding sites were blocked in 5 % milk in TBS-T (10 mM Tris/HCl pH 7.5, 150 mM NaCl, 0.05 % Tween 20). Polyclonal antibodies against NF-κB/RelA (sc-372, Santa Cruz, Santa Cruz, CA) or GAPDH (#5G4, HyTest, Finland) were incubated in the blocking solution or in 5 % BSA/TBS-T at 4 °C overnight. Antibody-bound proteins were detected using a horseradish peroxidase-coupled secondary antibody (anti-rabbit-IgG; Promega, Madison, WI).

Oxyblot analysis. Protein lysates from total liver were analyzed using the Oxyblot technology as previously described [21]. Briefly, after derivatization with hydrazide-biotin (Pierce), proteins were acetone precipitated and afterwards dissolved in 100 mM NaOH. Carbonylated proteins were detected by Westernblot analysis using horseradish peroxidase-coupled streptavidin (R&D Systems; Minneapolis, MN).

Histology and histomorphometry. Murine and routinely processed human liver samples were fixed in 4 % PFA in PBS overnight and embedded in paraffin. Analysis of human liver tissues was approved by the local ethics committee ("Kantonale Ethikkommission Zürich", application number StV26/2005 and KEK-ZH-Nr. 2013-0382). Sections (2 or 3.5 µm) were stained with hematoxylin/eosin (H&E) or Sirius Red (Sigma) and photographed (4 pictures/animal). Fibrotic tissue areas were manually determined using histomorphometry.

Immunohistochemistry and immunofluorescence. Paraffin sections (2 or 3.5 µm) from tissue that had been fixed in 4 % PFA or 95 % ethanol/1 % acetic acid were incubated for 45 min in 12 % BSA in PBS/0.025 % NP40/10 % NaN_3 to block unspecific binding sites. Sections were incubated with the primary antibody diluted in blocking buffer overnight at 4 °C. After application of a secondary antibody for 1 h, they were stained using the Vectastain Peroxidase Kit (Vector Laboratories, Burlingame, CA), counterstained with hematoxylin, rehydrated, and mounted with Mowiol. Alternatively, stainings were performed using a Ventana

staining platform (Roche, Rotkreuz, Switzerland). Sections were photographed using a Zeiss Imager.A1 microscope equipped with an Axiocam MRm camera and EC Plan-Neofluar objectives (10x/0.3, 20x/0.5). For data acquisition we used the Axiovision 4.6 software (all from Carl Zeiss, Inc., Oberkochen, Germany). Positive cells were quantified using the Image J software (Rasband WS, US NIH, Bethesda, MA). Antibodies used are listed in Supplementary Materials.

Detection and quantification of proliferating or apoptotic cells. Mice were injected *i.p.* with 5-bromo-2'-deoxyuridine (BrdU) (250 mg/kg body weight) and sacrificed 2 h after injection. Liver tissue was fixed in 95 % EtOH/1 % acetic acid overnight. BrdU positive cells were detected using a peroxidase-coupled antibody directed against BrdU (Roche). Apoptotic cells were identified by TUNEL staining using the cell death detection kit (Roche). Stained sections were photographed (4 pictures/animal), and positive and negative cells were counted manually using the Image J software.

Statistical analysis. Statistical analysis was performed using the GraphPad Prism5.0a software. *p*-values are two-tailed and were calculated using a regular Two-way ANOVA. Fisher's exact test was used to calculate the significance of tumor formation in female versus male mice using QuickCalcs (GraphPad). P values < 0.05 were considered statistically significant.

Results

Generation of mice lacking Nrf2 and p65/RelA in hepatocytes

To unravel a possible cross-talk between Nrf2 and NF-κB signaling in the liver, we generated mice lacking Nrf2 in all cells and p65/RelA in hepatocytes. In the double mutant AlbCre_p65/Nrf2ko mice hepatocytes are deficient in both Nrf2 and p65/RelA. qRT-PCR analysis verified the loss of *Nrf2* and/or reduction in *p65/RelA* expression, respectively, in samples from total liver of the double or single knockout mice (Fig. 1A,B). The complete loss of Nrf2 in AlbCre_Nrf2ko and AlbCre_p65/Nrf2ko mice was confirmed by semiquantitative PCR (Fig. 1B, right panel). Westernblot analysis demonstrated a strong reduction in p65/RelA levels in AlbCre_p65 and AlbCre_p65/Nrf2ko mice (Fig. 1C). The residual p65 expression occurs in non-parenchymal cells of the liver, including endothelial cells, as shown by immunofluorescence analysis (Fig. 1D).

Simultaneous loss of Nrf2 and p65/RelA in hepatocytes induces spontaneous liver damage

AlbCre_p65/Nrf2ko mice did not display obvious macroscopic abnormalities at the age of 8 weeks and they had a normal body weight (data not shown). As previously demonstrated [7], *Nrf2* knockout mice had a significant reduction in the liver-to-body weight ratio. This phenotype was, however, not aggravated by additional loss of p65 (Fig. 2A). Analysis of serum activities for aspartate transaminase (AST) and alanine transaminase (ALT) indicated lack of liver

damage in single and double knockout mice (Fig. 2B and data not shown). The number of TUNEL-positive apoptotic cells was also not significantly altered (Fig. 2C). Histological analysis of H&E stained liver sections showed that the overall liver morphology was not affected. However, focal accumulation of inflammatory cells was seen in the liver of AlbCre_p65ko mice and even more in AlbCre_p65/Nrf2ko mice (Fig. 2D, right picture in lower panel). In most cases this was accompanied by necrosis in the immediate environment (data not shown). Immunohistochemical analysis of liver sections showed a slight, but non-significant increase in the number Ly6G-positive neutrophils and of CD3-positive T cells in AlbCre_p65/Nrf2ko mice compared to controls (Fig. 2E).

Progressive liver damage and fibrosis in mice lacking Nrf2 and p65/RelA in hepatocytes

To determine the long-term consequences of Nrf2 and p65/RelA deletion in hepatocytes, we analyzed mice at 6 months of age. At this age, AlbCre_Nrf2ko and AlbCre_p65/Nrf2ko mice still showed a reduced liver-to-body weight ratio (Fig. 3A). There was only a minor increase in serum AST activity in the double knockout mice (Fig. 3B). The number of TUNEL-positive apoptotic cells was increased in AlbCre_p65 and AlbCre_p65/Nrf2ko mice (Fig. 3C). Histopathological analysis of H&E stained liver sections revealed mild liver damage in AlbCre_p65ko and AlbCre_Nrf2ko mice and more severe damage combined with focal accumulation of inflammatory cells in AlbCre_p65/Nrf2ko

mice and the presence of fibrotic areas (Fig. 3D). This was confirmed by Sirius Red staining of collagen and histomorphometric quantification of the fibrotic areas (Fig. 3E). Immunohistochemical stainings for Ly6G (neutrophils), CD3 (T cells), CD68 (macrophages) and B220 (B cells) and subsequent quantification of the different immune cells revealed an increase in B and T lymphocytes in AlbCre_p65/Nrf2ko mice at this time point (Fig. 3F).

Formation of hepatocellular adenoma-like tumors in aged female mice lacking Nrf2 and p65/RelA in hepatocytes

At the age of 18 months, the reduction in liver-to-body weight ratio was not further aggravated in AlbCre_Nrf2ko and AlbCre_p65/Nrf2 ko mice (Fig.4A), but the overall liver damage had become more severe (Fig. 4B-G). AST activity in the serum of AlbCre_Nrf2ko and of AlbCre_p65/Nrf2ko was increased at this time point, although the difference was not statistically significant due to the rather high variation among animals (Fig. 4B). AlbCre_p65ko and in particular AlbCre_p65/Nrf2ko mice exhibited necrosis (Fig. 4C,D) and inflammation (Fig. 4C,E,F) in the liver, and the number of Ly6G-positive cells was significantly increased in AlbCre_p65/Nrf2ko mice compared to the other genotypes (Fig. 4E). Finally, fibrotic tissue was present (Fig. 4G).

Most interestingly, tumors were detected in 4 out of 11 female mice, but in none of the 13 male mice that we analyzed (* $p = 0.0311$) (Fig. 5A). Histopathological analysis of these tumors revealed strong similarities with the inflammatory

subtype of human hepatocellular adenoma (iHCA) (Fig. 5B). This was confirmed by immunohistochemical staining for markers that distinguish between different HCA subtypes [22,23]. Like human iHCA (Fig. 5B, upper panels), the mouse tumors showed dilated, teleangiectasia-like sinusoids as highlighted by staining with a collagen IV antibody. Staining with a cytokeratin antibody that detects bile ducts confirmed that tumors were devoid of bile ducts/portal tracts (Fig.5B, middle panel). Both the human and the mouse tumors revealed only few proliferating tumor cells as revealed by Ki-67 staining, whereas large numbers of proliferating inflammatory cells were present. Furthermore, the tumor cells were positive for phosphorylated STAT3 (p-STAT3), indicative of active Jak/Stat signaling. In contrast to the human situation, where mutations (most likely somatic mutations) are restricted to the tumors, p-STAT3 staining was also seen in the non-tumorigenic liver of AlbCre_p65/Nrf2ko mice. This is likely due to the fact that all hepatocytes are deficient for Nrf2 and p65. Additional characteristics of human iHCA were seen in the mouse tumors, including (i) no loss of liver fatty acid binding protein (L-FABP), (ii) lack of nuclear β-catenin, (iii) lack of overexpression of the β-catenin target glutamine synthase (Fig. 5B, lower panel), and (iv) strong staining for serum amyloid A1 (SAA1) (Supplementary Figure S1).

We next stained human iHCAs with antibodies against (activated) p-NRF2 and/or p65. Consistent with the situation in the mouse tumors, iHCAs were mostly negative for p-NRF2, with the exception of very rare positive hepatocytes mostly at the tumor border and around pseudo-portal tracts, whereas widespread nuclear p-NRF2 reactivity was detectable in the peritumoral tissue, including in

stromal cells, in particular immune cells, and in proliferating bile ducts (Fig. 6A). A similar result was obtained for NF-κB/p65: There was a strong staining in peritumoral cells, including immune cells, whereas the iHCA tumor cells were negative for nuclear p65 (Fig. 6B). Taken together, these results demonstrate that a deficiency in activated NF-κB/p65 and NRF2 is also a hallmark of human iHCA.

Loss of p65 does not affect the expression of Nrf2 target genes involved in ROS defense

The progressive liver damage that we observed in the AlbCre_p65/Nrf2ko mice, but not in the single knockout mice, suggested that both transcription factors have partially redundant cytoprotective functions in the liver. To assess potential collaborative roles in the antioxidant defense, we first analyzed the levels of carbonylated proteins as a parameter for ROS-induced cell damage. Oxyblot analyses showed that several carbonylated proteins were present at higher levels in AlbCre_Nrf2ko compared to AlbCre and AlbCre_p65ko mice, but additional loss of p65/RelA did not enhance this effect (Supplementary Fig. S2). Consistent with this finding, several Nrf2 target genes involved in the cellular antioxidant defense system were expressed at lower levels in *Nrf2* knockout mice compared to wild-type controls, but their expression was not further reduced in the absence of p65. These include the genes encoding Nqo1 (*Nqo1*), glutathione S-transferase A2 (*Gsta2*), the glutathione biosynthesis enzyme glutamate

cysteine ligase catalytic subunit (*Gclc*), and the ROS-detoxifying enzyme peroxiredoxin 1 (*Prdx1*) (Fig. 7). Furthermore, there was no additive effect of Nrf2 and p65 deficiency on the expression of aldehyde oxidase 1, carbonyl reductase 3, peroxiredoxin 6 and epoxide hydrolase 1 (data not shown). The only exception was sulfiredoxin 1 (*Srxn1*), which was further repressed in the absence of p65 (Fig. 7). Overall, this finding suggests that Nrf2 and NF-κB regulate different genes in the liver and that the combined alteration in the expression of these different target genes leads to the observed liver pathology.

Discussion

We provide genetic evidence for an important collaborative function of Nrf2 and NF-κB in the control of liver homeostasis. While the absence of either Nrf2 or p65/RelA had no or only minor effects on liver morphology and function, simultaneous loss of both transcription factors caused progressive inflammation, followed by fibrosis and development of tumors resembling human iHCA.

It has previously been shown that Nrf2 affects NF-κB activity and *vice versa*. For example, Nrf2 activating compounds attenuated NF-κB activation in response to lipopolysaccharide [24] or carbon tetrachloride [25]. Furthermore, activation of Nrf2 by phenethyl isothiocyanate or sulforaphane inhibited phosphorylation of the inhibitor of NF-κB and subsequent nuclear translocation of p65, thereby inhibiting NF-κB signaling [26]. However, off-target effects of the Nrf2 activating compounds could not be excluded in these experiments. Though, studies with *Nrf2* knockout mice also argue for an effect of Nrf2 on NF-κB activity. Thus, Nrf2 ablation accelerated NF-κB mediated pro-inflammatory reactions [27], and Nrf2 deletion enhanced NF-κB DNA binding in the liver after PH [7]. However, direct evidence for a functional interplay of Nrf2 and NF-κB *in vivo* was still missing. The results obtained in the present study therefore provide the first genetic evidence for this cross-talk in the liver.

Consistent with our previous findings [7], a reduction of the cellular antioxidant defense capacity was observed in the liver of *Nrf2* knockout mice as reflected by the increase in oxidized proteins and the reduced expression of various genes

with a direct or indirect role in ROS defense. However, this was not further aggravated by the loss of p65, suggesting that Nrf2 and p65 regulate different sets of genes with different roles in cytoprotection. Of particular interest in this context are genes encoding anti-apoptotic proteins, which are under control of NF-κB [28-33]. Interestingly, lack of p65 in hepatocytes sensitized hepatocytes to pro-apoptotic stimuli such as TNF-α or lipopolysaccharide [13,15], and this was inhibited by administration of antioxidants [15]. Thus, in the absence of Nrf2 and the associated increase in ROS levels, the pro-apoptotic effect of a loss of NF-κB could be aggravated. Consistent with this assumption, Nrf2 deficiency enhanced the sensitivity of hepatocytes to TNF-α induced apoptosis *in vivo,* resulting in the development of severe hepatitis [34]. Since significant apoptosis was only detected in aged AlbCre_p65/Nrf2ko mice, this possibility, however, is unlikely the primary cause for the spontaneous inflammation seen in young AlbCre_p65/Nrf2ko mice. The latter may involve non cell-autonomous mechanisms, such as induction of cytokines or other mediators in the absence of Nrf2 and NF-κB in hepatocytes, which initiate an inflammatory response. The additional loss of Nrf2 in non-parenchymal cells may further aggravate such an effect, and future studies using mice lacking Nrf2 and p65 only in hepatocytes will clarify this issue.

The onset of inflammation in AlbCre_p65/Nrf2ko mice was first reflected by an increase in intrahepatic lymphocytes. This may suggest that hepatocytes deficient in Nrf2 and NF-κB/p65 are recognized by cells of the adaptive immune system, possibly due to presentation of as yet uncharacterized antigens. At later

stages, a significant increase in neutrophils and macrophages was also observed. Similar to chronic hepatitis in humans, the inflammatory response was followed by the development of liver fibrosis. In the future, it will therefore be interesting to determine the expression/activation of both NRF2 and NF-κB in fibrotic and cirrhotic human liver.

Interestingly, a significant fraction of aged female, but not of male AlbCre_p65/Nrf2ko mice developed lesions that share various features with human iHCA, a rare benign primary liver cell tumor [35]. HCAs comprise a heterogenous group of tumors characterized by specific phenotypic and genetic alterations. Currently, they are divided into 4 subtypes: (a) iHCA, (b) HCAs with mutations in the gene encoding hepatocyte nuclear factor 1α, (c) HCAs with mutations in the β-catenin gene and (d) "unclassified" HCA without known genetic alterations [36]. The tumors in our mutant mice showed various similarities to human iHCA at the histological and immunohistochemical level. iHCA accounts for 30-40% of all HCAs and occurs predominantly in young women, who use oral contraceptives with high estrogen content and often exhibit a systemic inflammatory condition [37]. Therefore, the exclusive detection of the iHCA-like lesions in female mice is of particular interest and raises the intriguing possibility that estrogens may affect the response of liver cells to Nrf2 and NF-κB deficiency.

Approximately 90% of iHCAs in humans are characterized by somatic activating mutations in the gene encoding interleukin-6 (IL-6) signal transducer/gp130, or in

additional genes that result in activation of STAT3 in an IL-6-independent manner [38,39,40]. iHCAs also display overexpression of CCL20, accounting for the recruitment of inflammatory cells to the lesions [39,41]. It is as yet unclear if these mutations are causative or only required for the progression of the tumors. A role of NRF2 and NF-κB in the pathogenesis of iHCA has as yet not been demonstrated, and mutations in these genes have not been detected in human iHCA [40]. However, our finding that simultaneous deficiency in Nrf2 and p65 in murine hepatocytes is sufficient to activate Stat3 and to initiate the development of liver tumors reminiscent of human iHCA, raised the question of a possible deficiency in one or both of these transcriptions factors in human iHCA. Indeed, the tumor cells of five analyzed human HCAs did not show immunoreactivity for nuclear p-NRF2 and NF-κB/p65, suggesting that a deficiency in the expression and/or activation of these important cytoprotective transcription factors is also a hallmark of human iHCA and may contribute to the pathogenesis of this type of tumor.

Although benign, iHCAs can become life-threatening due to bleeding, which occurs in 30% of these tumors. Furthermore, up to 10% of iHCA, in particular those harboring β-catenin mutations, progress to hepatocellular carcinomas [22,42]. Thus, identification of novel strategies for the prevention and/or treatment of HCA is of strong medical interest, and the findings described in this study suggest that activation of NRF2 and/or NF-κB could be a promising strategy in patients diagnosed with HCA or in high-risk female and/or obese patients.

Acknowledgements

We thank Dominik Schwitter, ETH Zurich, Christiane Mittmann and André Fitsche, (both from the University Hospital Zurich) for excellent technical assistance and Dr. Yuet-Wai Kan, University of California, San Francisco, for the *Nrf2* knockout mice.

References

[1] Schwabe RF, Brenner DA. Mechanisms of liver injury. I. TNF-alpha-induced liver injury: Role of IKK, JNK, and ROS pathways. Am J Physiol Gastrointest Liver Physiol 2006;290:G583-589.

[2] Luedde T, Beraza N, Kotsikoris V, van Loo G, Nenci A, De Vos R, et al. Deletion of NEMO/IKKgamma in liver parenchymal cells causes steatohepatitis and hepatocellular carcinoma. Cancer Cell 2007;11(2):119-132.

[3] Choi J, Corder NL, Koduru B and Wang Y. Oxidative stress and hepatic Nox proteins in chronic hepatitis C and hepatocellular carcinoma. Free Radic Biol Med 2014;72:267-284.

[4] Sykiotis GP, Bohmann D. Stress-activated Cap'n'Collar transcription factors in aging and human disease. Sci Signal 2010;3:re3.

[5] Shin SM, Yang JH, Ki SH. Role of the Nrf2-ARE pathway in liver diseases. Oxid Med Cell Longev 2013;2013:763257.

[6] Aleksunes LM and Manautou JE. Emerging role of Nrf2 in protecting against hepatic and gastrointestinal disease. Toxicol Pathol 2007;35(4):459-473.

[7] Beyer TA, Xu W, Teupser D, auf dem Keller U, Bugnon P, Hildt E, et al. Impaired liver regeneration in Nrf2 knockout mice: Role of ROS-mediated insulin/IGF-1 resistance. EMBO J 2008;27:212-223.

[8] Wakabayashi N, Shin S, Slocum SL, Agoston ES, Wakabayashi J, Kwak M-K, et al. Regulation of Notch1 signaling by Nrf2: Implications for tissue regeneration. Sci Signal 2010;3(130):ra52

[9] Xu W, Hellerbrand C, Köhler U, Bugnon P, Kan Y, Werner S, et al. The Nrf2 transcription factor protects from toxin-induced liver injury and fibrosis. Lab Invest 2008;88:1068-1078

[10] Schreck R, Rieber P, Baeuerle PA. Reactive oxygen intermediates as apparently widely used messengers in the activation of the NF-kappa B transcription factor and hiv-1. EMBO J 1991;10:2247-2258.

[11] Chaisson ML, Brooling JT, Ladiges W, Tsai S, Fausto N. Hepatocyte-specific inhibition of NF-kappaB leads to apoptosis after TNF treatment, but not after partial hepatectomy. J Clin Invest 2002;110:193-202.

[12] Iimuro Y, Nishiura T, Hellerbrand C, Behrns KE, Schoonhoven R, Grisham JW, et al. NFkappaB prevents apoptosis and liver dysfunction during liver regeneration. J Clin Invest 1998;101:802-811.

[13] Luedde T, Heinrichsdorff J, de Lorenzi R, de Vos R, Roskams T, Pasparakis M. IKK1 and IKK2 cooperate to maintain bile duct integrity in the liver. PNAS 2008;105:9733-9738.

[14] Pereira SG, Oakley F. Nuclear factor-kappaB1: Regulation and function. Int J Biochem Cell Biol 2008;40:1425-1430.

[15] Geisler F, Algül H, Paxian S, Schmid RM. Genetic inactivation of RelA/p65 sensitizes adult mouse hepatocytes to tnf-induced apoptosis in vivo and in vitro. Gastroenterology 2007;132:2489-2503.

[16] Keum Y-S, Han Y-H, Liew C, Kim J-H, Xu C, Yuan X, et al. Induction of heme oxygenase-1 (HO-1) and NAD[P]H: Quinone oxidoreductase 1 (NQO1) by a phenolic antioxidant, butylated hydroxyanisole (BHA) and its metabolite, tert-butylhydroquinone (tBHQ) in primary-cultured human and rat hepatocytes. Pharm Res 2006;23:2586-2594.

[17] Yuan X, Xu C, Pan Z, Keum Y-S, Kim J-H, Shen G, et al. Butylated hydroxyanisole regulates are-mediated gene expression via Nrf2 coupled with Erk and Jnk signaling pathway in HepG2 cells. Mol Carcinog 2006;45:841-850.

[18] Chan K, Lu R, Chang JC, Kan YW. Nrf2, a member of the NFE2 family of transcription factors, is not essential for murine erythropoiesis, growth, and development. Proc Natl Acad Sci USA 1996;93:13943-13948.

[19] Chomczynski P, Sacchi N. Single-step method of RNAa isolation by acid guanidinium thiocyanate-phenol-chloroform extraction. Anal Biochem 1987;162:156-159.

[20] Koegel H, von Tobel L, Schäfer M. Albert S, Kremmer E, Mauch C et al. Loss of serum response factor in keratinocytes results in hyperproliferative skin disease in mice. J Clin Invest 2009;119:899-910.

[21] Hensley K. Detection of protein carbonyls by means of biotin hydrazide-streptavidin affinity methods. Methods Mol Biol 2009;536:457–462.

[22] Bioulac-Sage P, Balabaud C, Zucman-Rossi J. Focal nodular hyperplasia, hepatocellular adenomas: Past, present, future. Gastroenterol Clin Biol 2010;34:355-358.

[23] Bioulac-Sage P, Cubel G, Balabaud C, Zucman-Rossi J. Revisiting the pathology of resected benign hepatocellular nodules using new immunohistochemical markers. Semin Liver Dis 2011;31:91-103.

[24] Jeong W-S, Kim I-W, Hu R, Kong A-NT. Modulatory properties of various natural chemopreventive agents on the activation of NF-kappaB signaling pathway. Pharm Res 2004;21:661-670.

[25] Reyes-Gordillo K, Segovia J, Shibayama M, Vergara P, Moreno MG, Muriel P. Curcumin protects against acute liver damage in the rat by inhibiting NF-kappaB, proinflammatory cytokines production and oxidative stress. Biochim Biophys Acta 2007;1770:989-996.

[26] Xu C, Shen G, Chen C, Gélinas C, Kong A-NT. Suppression of NF-kappaB and NF-kappaB-regulated gene expression by sulforaphane and PEITC through ikappabalpha, IKK pathway in human prostate cancer PC-3 cells. Oncogene 2005;24:4486-4495.

[27] Li W, Khor TO, Xu C, Shen G, Jeong W-S, Yu S, et al. Activation of Nrf2-antioxidant signaling attenuates NFkappaB-inflammatory response and elicits apoptosis. Biochem Pharmacol 2008;76:1485-1489.

[28] Catz SD, Johnson JL. Transcriptional regulation of Bcl-2 by nuclear factor kappa B and its significance in prostate cancer. Oncogene 2001;20:7342-7351.

[29] Kreuz S, Siegmund D, Scheurich P, Wajant H. NF-kappaB inducers upregulate cFlip, a cycloheximide-sensitive inhibitor of death receptor signaling. Mol Cell Biol 2001;21:3964-3973.

[30] Lee HH, Dadgostar H, Cheng Q, Shu J, Cheng G. NF-kappaB-mediated up-regulation of Bcl-x and Bfl-1/a1 is required for CD40 survival signaling in B lymphocytes. Proc Natl Acad Sci USA 1999;96:9136-9141.

[31] Stehlik C, de Martin R, Binder BR, Lipp J. Cytokine induced expression of porcine inhibitor of apoptosis protein (IAP) family member is regulated by NF-kappa B. Biochem Biophys Res Commun 1998;243:827-832.

[32] Stehlik C, de Martin R, Kumabashiri I, Schmid JA, Binder BR, Lipp J. Nuclear factor (NF)-kappaB-regulated X-chromosome-linked IAP gene expression protects endothelial cells from tumor necrosis factor alpha-induced apoptosis. J Exp Med 1998;188:211-216.

[33] You M, Ku PT, Hrdlicková R, Bose HR. Ch-IAP1, a member of the inhibitor-of-apoptosis protein family, is a mediator of the antiapoptotic activity of the v-rel oncoprotein. Mol Cell Biol 1997;17:7328-7341.

[34] Morito N, Yoh K, Itoh K, Hirayama A, Koyama A, Yamamoto M, et al. Nrf2 regulates the sensitivity of death receptor signals by affecting intracellular glutathione levels. Oncogene 2003;22(58):9275-9281.

[35] Bühler H, Pirovino M, Akobiantz A, Altorfer J, Weitzel M, Maranta E, et al. Regression of liver cell adenoma. A follow-up study of three consecutive patients after discontinuation of oral contraceptive use. Gastroenterology 1982;82:775-782.

[36] Bioulac-Sage P, Blanc JF, Rebouissou S, Balabaud C, Zucman-Rossi J. Genotype phenotype classification of hepatocellular adenoma. World J Gastroenterol 2007;13:2649-2654.

[37] Bioulac-Sage P, Laumonier H, Laurent C, Zucman-Rossi J, Balabaud C. Hepatocellular adenoma: What is new in 2008. Hepatol Int 2008;2:316-321.

[38] Rebouissou S, Amessou M, Couchy G, Poussin K, Imbeaud S, Pilati C, et al. Frequent in-frame somatic deletions activate gp130 in inflammatory hepatocellular tumours. Nature 2009;457:200-204.

[39] Spannbauer MM, Trautwein C. Frequent in-frame somatic deletions activate gp130 in inflammatory hepatocellular tumors. Hepatology 2009;49:1387-1389.

[40] Pilati C, Letouzé E, Nault JC, Imbeaud S, Boulai A, Calderaro J et al. Genomic profiling of hepatocellular adenomas reveals recurrent FRK-activating mutations and the mechanisms of malignant transformation. Cancer Cell 2014;25(4):428-41.

[41] Schutyser E, Struyf S, Van Damme J. The cc chemokine CC0L20 and its receptor CCR6. Cytokine Growth Factor Rev 2003;14:409-426.

[42] Zucman-Rossi J, Jeannot E, Nhieu JTV, Scoazec J-Y, Guettier C, Rebouissou S, et al. Genotype-phenotype correlation in hepatocellular adenoma: New classification and relationship with HCC. Hepatology 2006;43:515-524.

Legends to Figures

Figure 1. Verification of the loss of p65/RelA and Nrf2 in hepatocytes. (A,B) RNA from total liver of AlbCre, AlbCre_p65ko, AlbCre_Nrf2ko and AlbCre_p65/Nrf2ko mice was analyzed by qRT-PCR for expression of *p65* (A) and *Nrf2* (B, left panel) relative to *18s* RNA (N = 6 per genotype). Error bars represent mean ± s.d. *P*-values are two-tailed and were calculated using 2-way ANOVA. The tabular results are shown below each bar graph. Statistically significant differences are highlighted in bold. Nrf2 and 18sRNA PCR products were loaded on an agarose gel (B, right panel). (C) Total liver lysates (30 µg protein) were analyzed by immunoblotting for p65 and GAPDH (loading control). (D) Liver sections were analyzed by immunofluorescence for p65 (red); nuclei were counterstained with DAPI (blue). Note the remaining p65 staining in blood vessels of AlbCre_p65ko mice. Bar: 50 µm.

Figure 2. Lack of p65 and Nrf2 in hepatocytes induces focal liver damage. Mice were analyzed at the age of 2 months. (A) Liver-to-body weight ratio in AlbCre, AlbCre_p65ko, AlbCre_Nrf2ko and AlbCre_p65/Nrf2ko mice (N = 10 per genotype). (B) AST activity in the serum (N = 4). (C) TUNEL-positive (apoptotic cells) in liver sections (N = 5 per genotype). (D) Representative H&E-stained liver sections (out of 10 mice per genotype). Bars: 100 µm. (E) Numbers of Ly6G- and CD3-positive cells per area in liver sections (N = 5 per genotype). Error bars

represent mean ± s.d. *p*-values are two-tailed and were calculated using a regular 2-way ANOVA. The tabular results are shown below each bar graph.

Figure 3. Progressive inflammation and fibrosis in AlbCre_p65/Nrf2ko mice. Mice were analyzed at the age of 6 months. (A) Liver-to-body weight ratio (N = 10 per genotype). (B) Serum activity of AST (N = 4 per genotype). (C) TUNEL-positive (apoptotic) cells in liver sections (N = 5 per genotype). (D,E) Representative H&E- or Sirius Red-stained liver sections from mice of all four genotypes. Bars: 100 µm. Bar graph in (E) shows area of fibrotic tissue as determined by histomorphometrical analysis of Sirius Red-stained sections (N = 5). (F) Ly-6G-, CD3-, CD68-, or B220-positive cells (N = 5 per genotype). Error bars represent mean ± s.d. *p*-values are two-tailed and were calculated using 2-way ANOVA. The tabular results are shown below each bar graph. Statistically significant differences are highlighted in bold.

Figure 4. Severe liver damage and fibrosis in aged p65/Nrf2-deficient mice. Mice were analyzed at the age of 18 months. (A) Liver-to-body weight ratios (N = 10 per genotype). (B) Serum activity of AST (N = 4 per genotype). (C) Representative liver sections from mice of all genotypes stained with H&E. Bars: 100 µm. (D) Histological scoring of necrosis using H&E-stained liver sections, performed blinded by a liver pathologist. Scatter plot shows data points from individual mice. Score 0: no necrosis; Score 1: spotty necrosis; Score 2: confluent necrosis. (E) Numbers of Ly6G-positive cells in liver sections

determined by immunohistochemistry (N = 4 per genotype). (F) Inflammation scoring using H&E-stained liver sections, performed blinded by a liver pathologist. Score 0: no inflammation; Score 1: mild inflammation; Score 2: moderate inflammation; Score 3: strong inflammation. (G) Area of fibrotic tissue as determined by histomorphometrical analysis of Sirius Red-stained sections (N = 4). Error bars represent mean ± s.d. *p*-values are two-tailed and were calculated using 2-way ANOVA. The tabular results are shown below each bar graph. Statistically significant differences are highlighted in bold.

Figure 5. Aged female p65/Nrf2-deficient mice develop tumors resembling human iHCA. (A) Adenoma incidence in aged AlbCre_p65/Nrf2ko mice. Note the statistically significant difference in tumor formation between male and female mice according to Fisher's exact test. (B) Representative sections from a human iHCA adjacent to non-tumorigenic liver (upper row) and from a mouse lesion adjacent to non-tumorigenic liver, stained with H&E (black-filled arrowheads indicate lymphocyte infiltrates; white-filled arrowheads indicate dilated, teleangiectasia-like sinusoids) or immunostained for collagen IV, cytokeratin 7 (human) or pan-cytokeratin (mouse), Ki-67, p-STAT3, L-FABP, β-catenin (note the positive membrane staining, but the lack of nuclear staining) and glutamine synthase. Bars: 100 µm; 50 µm in inserts.

Fig. 6 Lack of nuclear p-NRF2 and NF-κB/p65 in the tumor cells of human iHCA. Representative sections from a human iHCA (T) adjacent to non-tumorous

liver (PT) immunostained with antibodies against p-NRF2 (A) or p65 (B). Higher magnifications of tumor cells or peri-tumoral tissue are shown in the left or right panels, respectively. Black arrowheads: bile ducts; white arrowheads: inflammatory cells. Bars: 200 µm (middle panel) or 100 µm (left and right panels).

Figure 7. Effect of Nrf2 and/or p65 deficiency on expression of Nrf2 target genes involved in ROS defense. RNA from total liver of 8 week-old mice was analyzed by qRT-PCR for the expression of the Nrf2 target genes *Srxn*, *Nqo1*, *Gsta2*, *Gclc* and *Prdx1* relative to *18s* rRNA (N = 3-5 per genotype). Error bars represent mean ± s.d. *p*-values are two-tailed and were calculated using 2-way ANOVA. The tabular results are shown below each bar graph. Statistically significant differences are highlighted in bold.

A

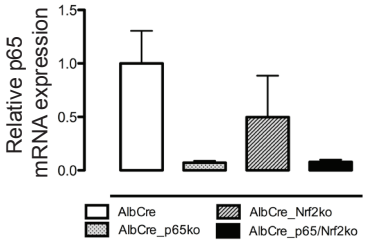

Source of variation	P value
Interaction	*0.0844*
Nrf2	*0.0857*
p65	***< 0.0001***

B

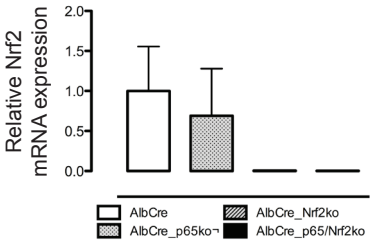

Source of variation	P value
Interaction	*0.8451*
Nrf2	***< 0.0001***
p65	*0.4745*

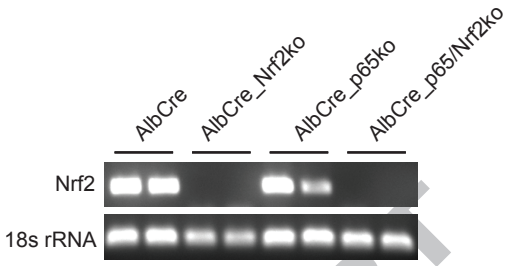

C

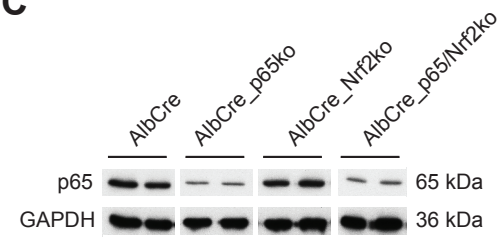

D

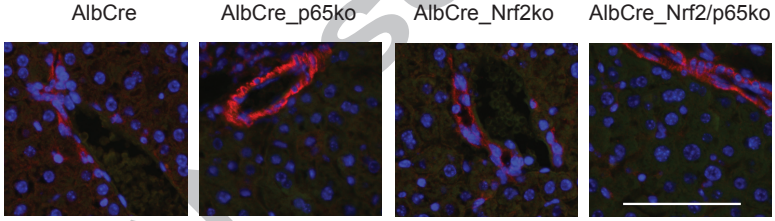

A

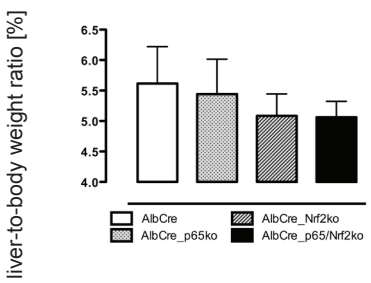

Source of variation	P value
Interaction	0.5966
Nrf2	0.0027
p65	0.4938

B

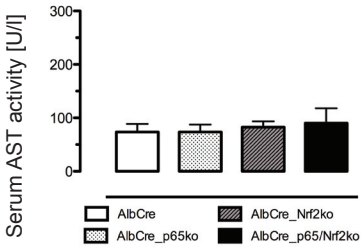

Source of variation	P value
Interaction	0.6873
Nrf2	0.1862
p65	0.6873

C

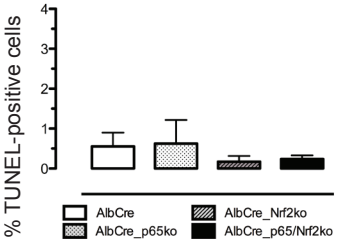

Source of variation	P value
Interaction	0.9908
Nrf2	0.0591
p65	0.7157

D

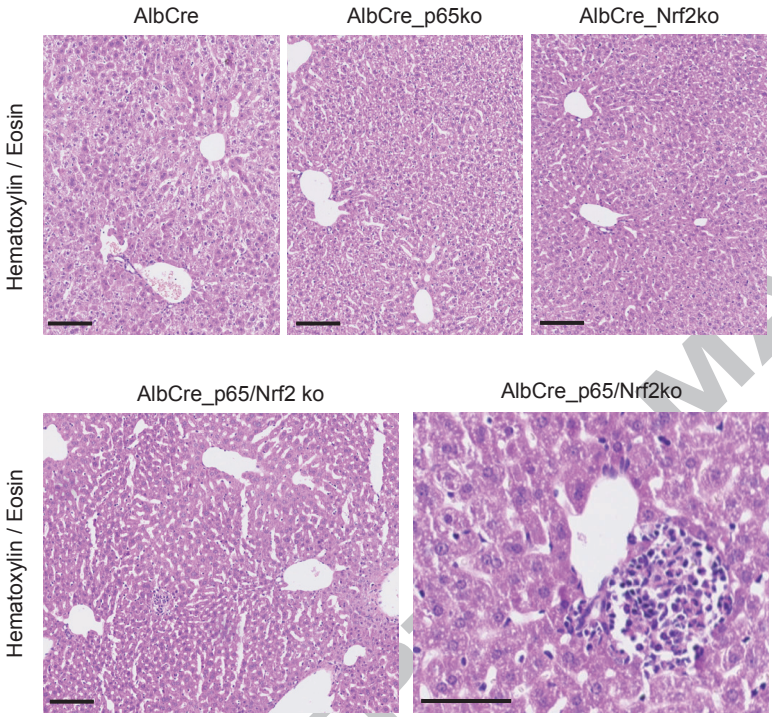

E

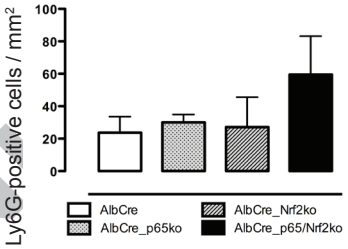

Source of variation	P value
Interaction	0.213
Nrf2	0.1243
p65	0.0765

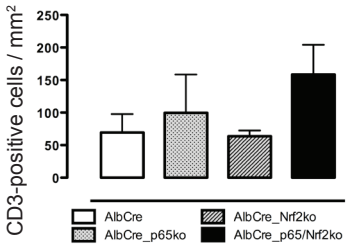

Source of variation	P value
Interaction	0.2889
Nrf2	0.3795
p65	0.0622

A

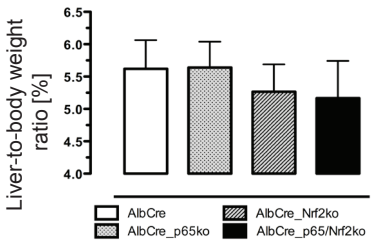

Source of variation	P value
Interaction	0.5054
Nrf2	**0.0288**
p65	0.5617

B

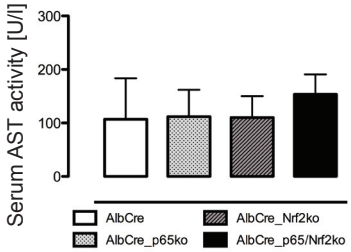

Source of variation	P value
Interaction	0.477
Nrf2	0.4083
p65	0.3789

C

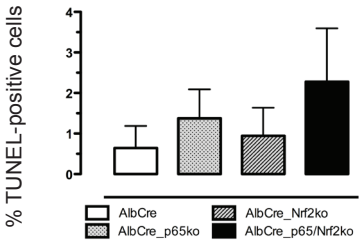

Source of variation	P value
Interaction	0.5175
Nrf2	0.2063
p65	**0.0393**

D

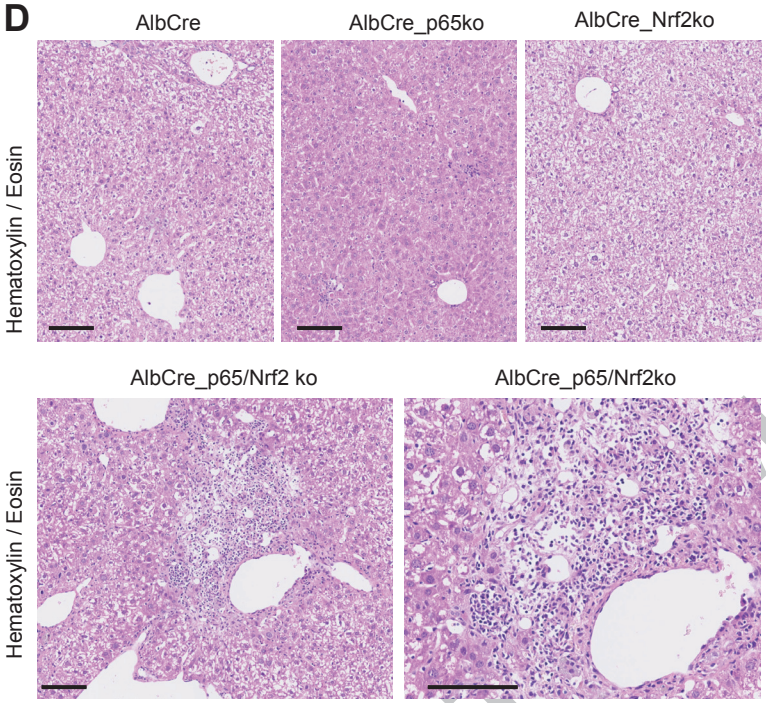

E

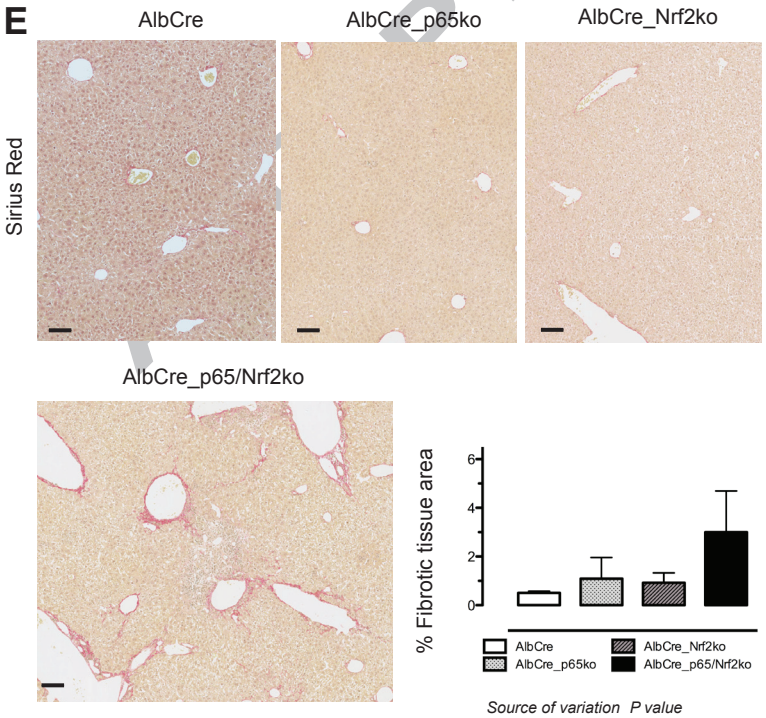

Source of variation	P value
Interaction	0.1479
Nrf2	**0.0311**
p65	**0.0152**

F

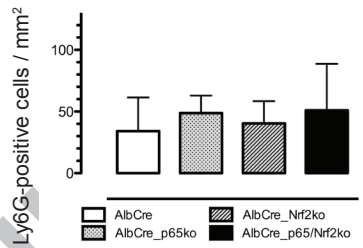

Source of variation	P value
Interaction	0.9915
Nrf2	0.917
p65	0.3395

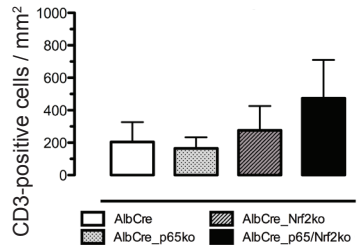

Source of variation	P value
Interaction	0.1563
Nrf2	**0.0292**
p65	0.336

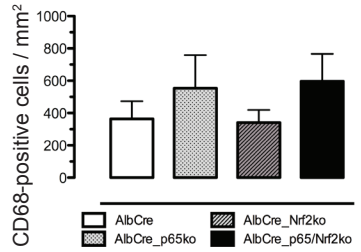

Source of variation	P value
Interaction	0.6567
Nrf2	0.8913
p65	**0.0085**

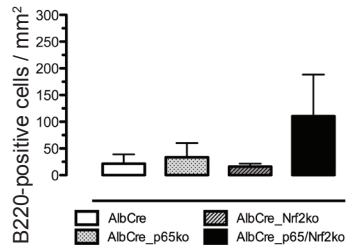

Source of variation	P value
Interaction	0.1634
Nrf2	0.223
p65	0.0801

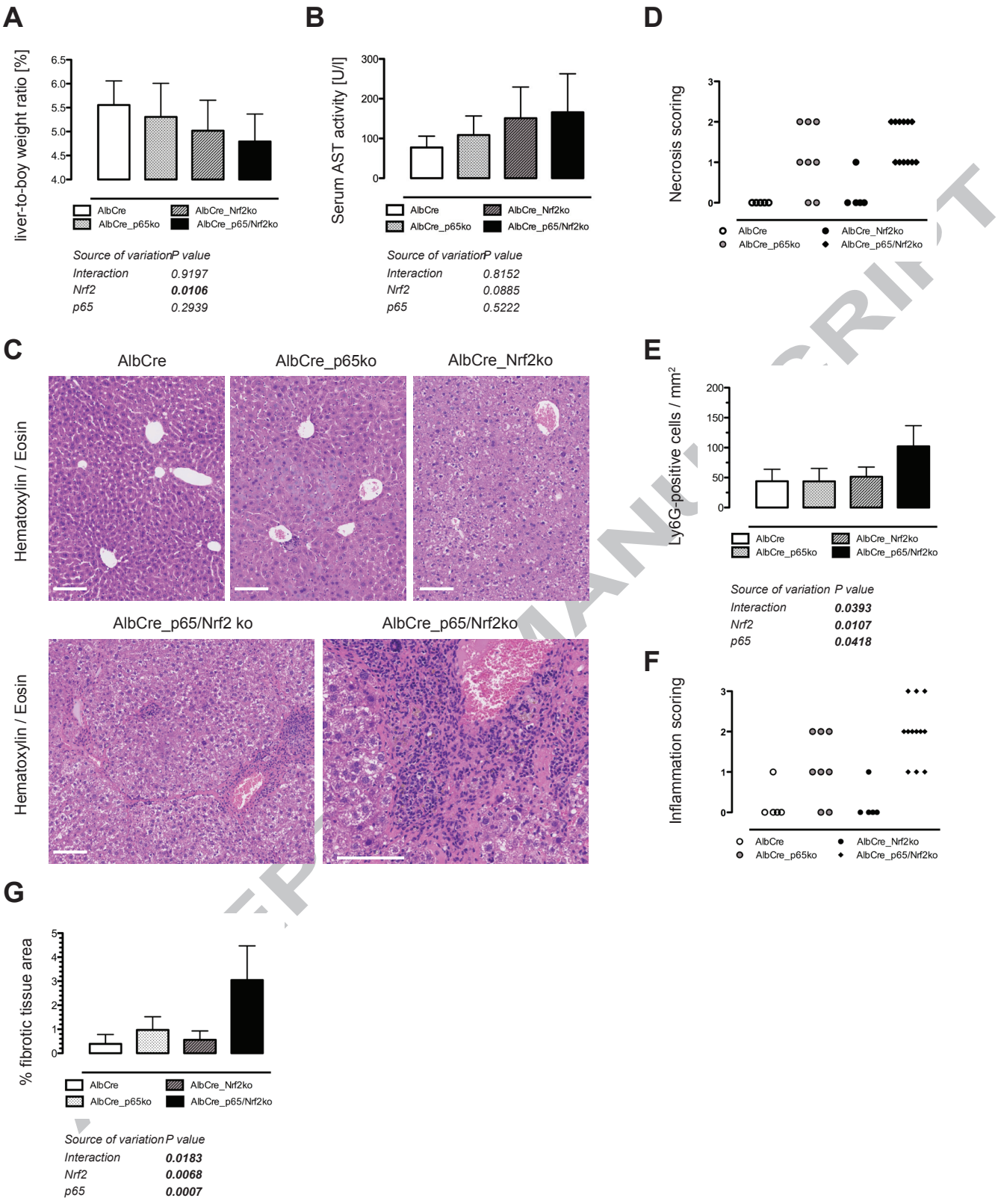

A

	iHCA-like tumors	No tumors	*Total*
Males	0	13	*13*
Females	4	7	*11*
Total	*4*	*20*	*24*

** p-Value 0.0311*

B

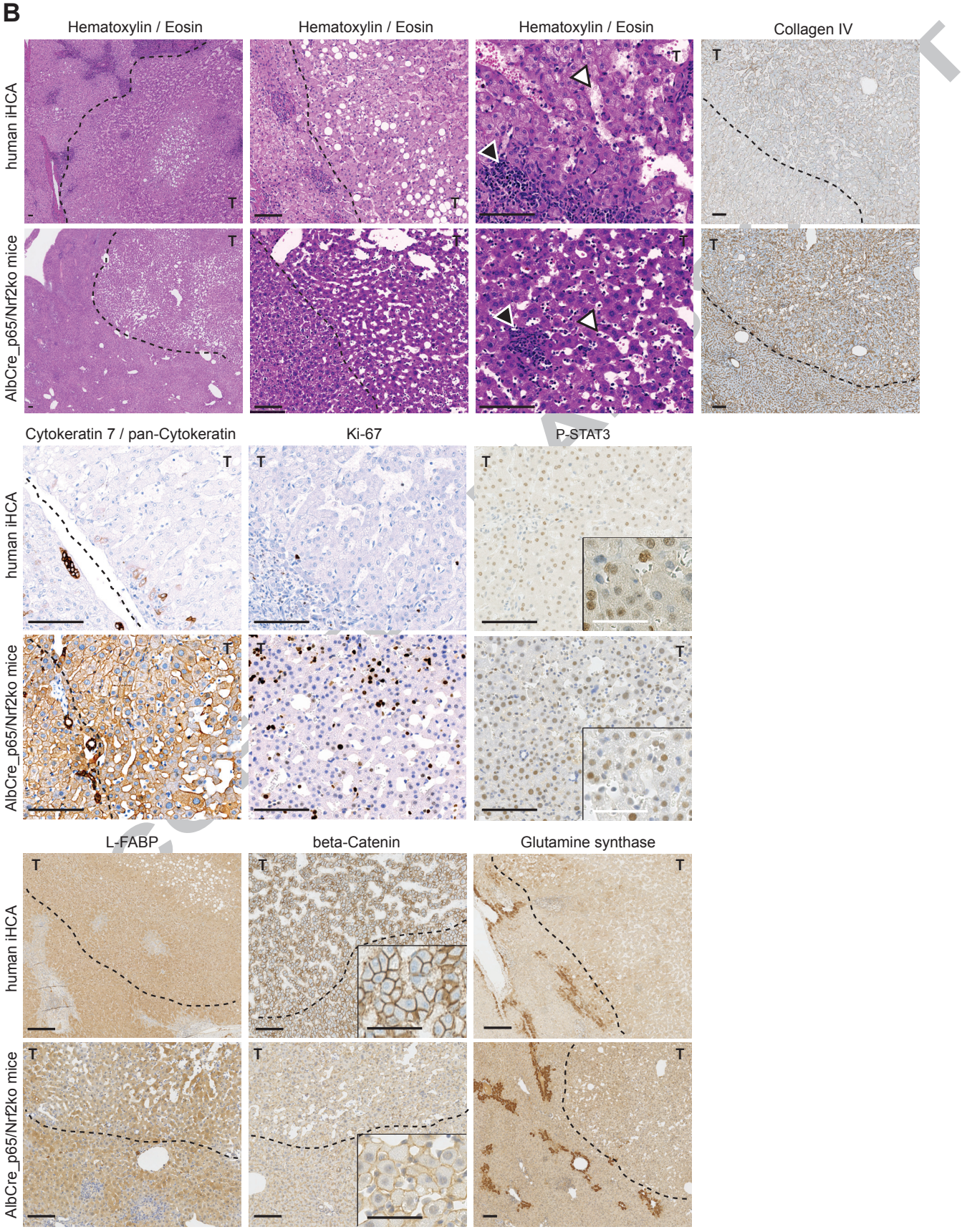

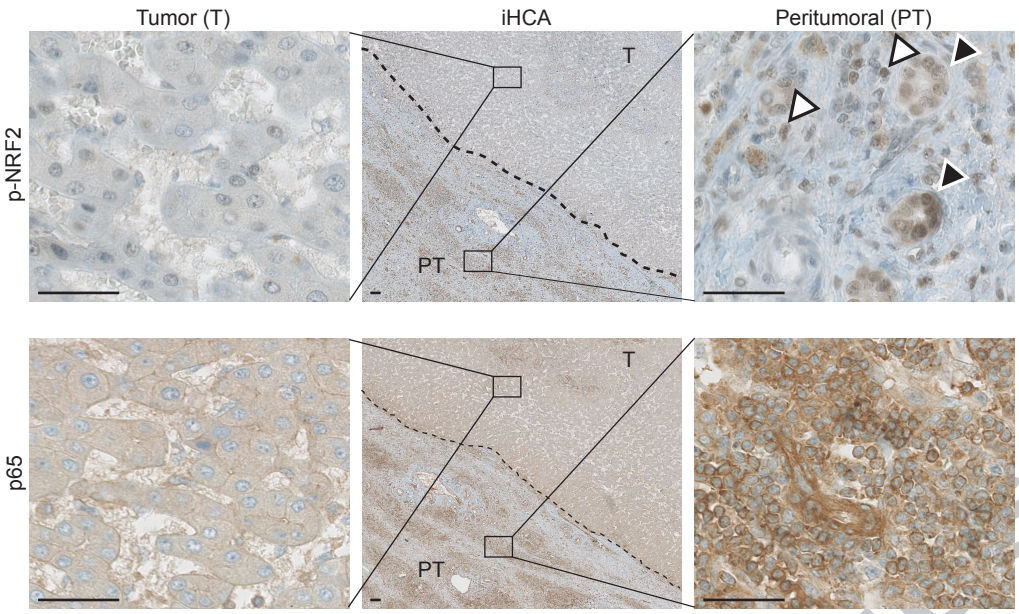

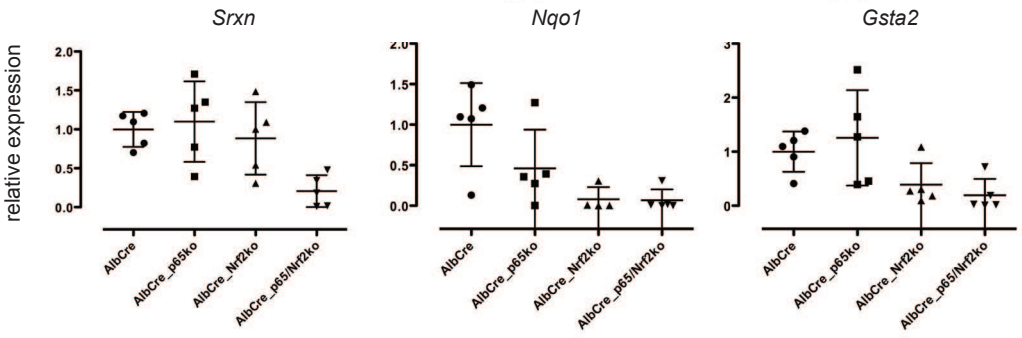

Source of variation	P value
Interaction	**0.0363**
Nrf2	**0.009**
p65	0.1089

Source of variation	P value
Interaction	0.1475
Nrf2	**0.0018**
p65	0.1319

Source of variation	P value
Interaction	0.3628
Nrf2	**0.0032**
p65	0.9028

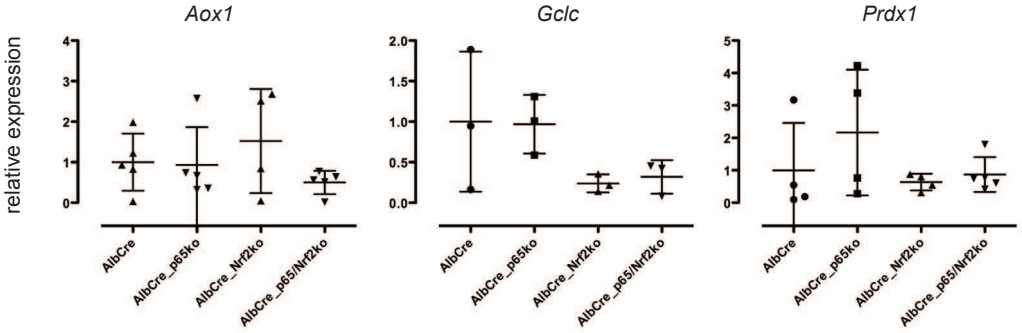

Source of variation	P value
Interaction	0.2409
Nrf2	0.9099
p65	0.1827

Source of variation	P value
Interaction	0.8452
Nrf2	**0.0353**
p65	0.9317

Source of variation	P value
Interaction	0.4438
Nrf2	0.1823
p65	0.2574

Köhler et al, Graphical Abstract

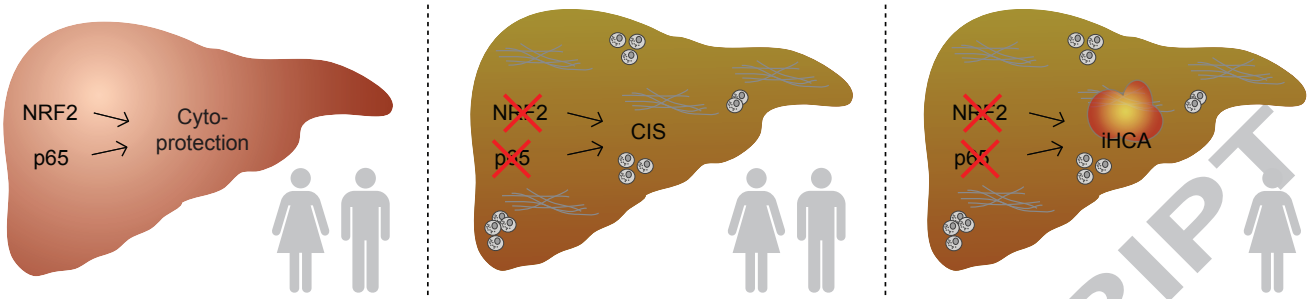

Normal liver

Chronic inflammatory state (CIS):
Inflammation and fibrosis

Inflammatory hepatocellular
adenoma (iHCA)